The Influence of UV–Ozone, O2 Plasma, and CF4 Plasma Treatment on the Droplet-Based Deposition of Diamond Nanoparticles

Peer-reviewed author version

VERDING, Pieter; MARY JOY, Rani; REENAERS, Dieter; SHANIVARASANTHE NITHYANANDA KUMAR, Rachith; ROUZBAHANI BAYATANI, Rozita; Jeunen, Ewoud; Thomas, Seppe; DESTA, Derese; BOYEN, Hans-Gerd; POBEDINSKAS, Paulius; HAENEN, Ken & DEFERME, Wim (2023) The Influence of UV–Ozone, O2 Plasma, and CF4 Plasma Treatment on the Droplet-Based Deposition of Diamond Nanoparticles. In: ACS Applied Materials & Interfaces, 16 (1) , p. 1719 -1726.

DOI: 10.1021/acsami.3c14014
Handle: http://hdl.handle.net/1942/42176

The influence of UV-ozone, O_2- and CF_4-plasma treatment on the droplet-based deposition of diamond nanoparticles

Journal:	*ACS Applied Materials & Interfaces*
Manuscript ID	am-2023-14014g.R2
Manuscript Type:	Article
Date Submitted by the Author:	n/a
Complete List of Authors:	Verding, Pieter; Hasselt University, Institute for Materials Research (IMO) Mary Joy, Rani; Hasselt University, Institute for Materials Research (IMO) Reenaers, Dieter; Hasselt University, Institute for Materials Research kumar, Rachith; Hasselt University, Engineering Technology Rouzbahani, Rozita; Hasselt University, Institute for Materials Research Jeunen, Ewoud; Hasselt University Thomas, Seppe; Hasselt University Desta, Derese; Hasselt University, Institute for Materials research (IMO) Boyen, Hans-Gerd; Hasselt University, Institute for Materials research (IMO) Pobedinskas, Paulius; Hasselt University, Haenen, Ken; Hasselt University, Institute for Materials Research (IMO) Deferme, Wim; Universiteit Hasselt, IMO-IMOMEC

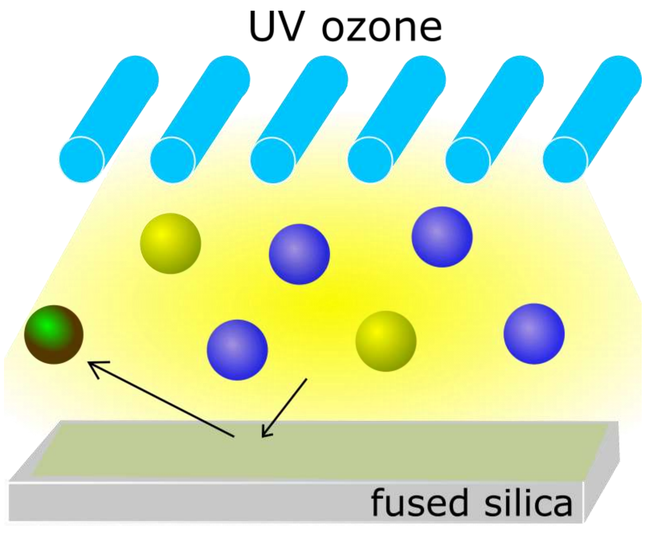

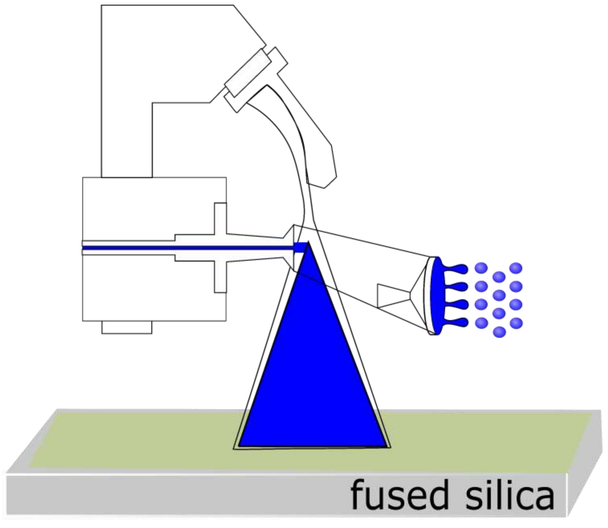

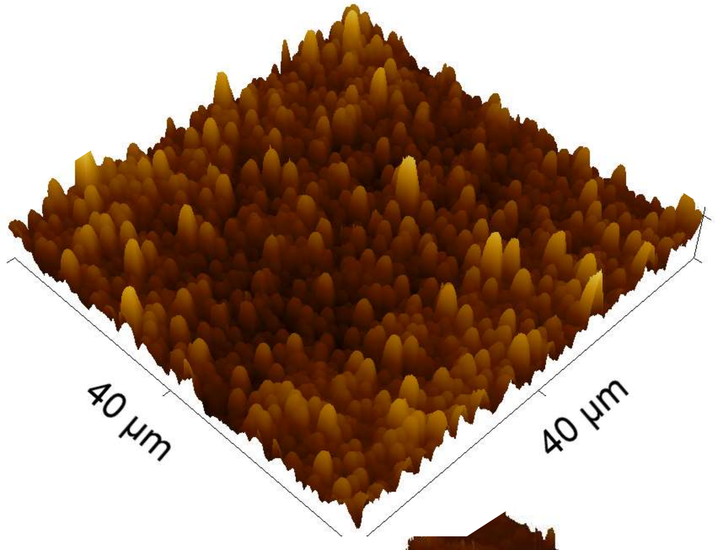

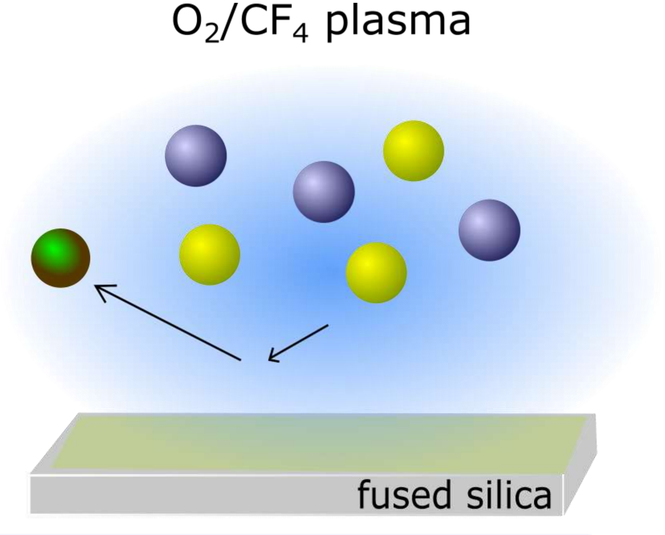

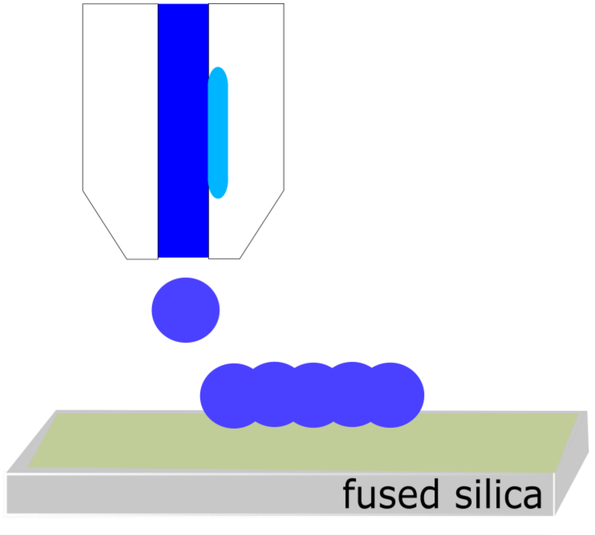

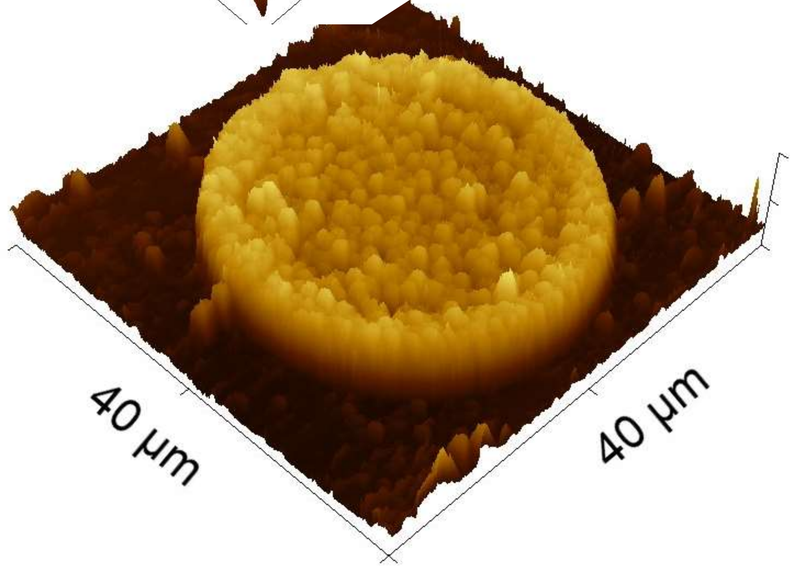

Surface treatment

Nano diamond seeding

Diamond coating/pattern

The influence of UV-ozone, O_2- and CF_4-plasma treatment on the droplet-based deposition of diamond nanoparticles

*Pieter Verding[1,2], Rani Mary Joy[1,2], Dieter Reenaers[1,2], Rachith Shanivarasanthe Nithyananda Kumar[1,2], Rozita Rouzbahani[1,2], Ewoud Jeunen[1], Seppe Thomas[1], Derese Desta[1,2], Hans-Gerd Boyen[1,2], Paulius Pobedinskas[1,2], Ken Haenen[1,2], Wim Deferme[1,2]**

[1] Hasselt University, Institute for Materials Research (IMO), Wetenschapspark 1, 3590 Diepenbeek, Belgium

[2] IMEC vzw, IMOMEC, Wetenschapspark 1, 3590 Diepenbeek, Belgium

* *Corresponding author: tel:+32 11 26 88 74, email: wim.deferme@uhasselt.be*

Keywords: UV-Ozone, O_2-plasma, CF_4-plasma, Ink-jet printing, Ultrasonic spray coating, pre-treatment, diamond nano-seeds

Abstract

Surface treatment is critical for homogeneous coating over a large area and high-resolution patterning of nanodiamond (ND) particles. To optimize the interaction between the surface of a

substrate and the colloid of ND particles, it is essential to remove hydrocarbon contamination by a surface treatment and to increase the surface energy of the substrate, hence improving the diamond film homogeneity upon its deposition. However, the impact of substrate surface treatment on the properties of coatings and patterns is not fully understood. This study explores the impact of UV-ozone, O_2, and CF_4 plasma treatments on the wetting properties of the fused silica glass substrate surface. We identify the optimal time interval between the treatment and subsequent ND coating/patterning processes, which were conducted using ink-jet printing and ultrasonic spray coating techniques. Our results showed that UV-ozone and O_2 plasma resulted in hydrophilic surfaces, while CF_4 plasma treatment resulted in hydrophobic surfaces. We demonstrate the use of CF_4 plasma treatment before ink-jet printing to generate high-resolution patterns with dots as small as 30 μm in diameter. Ultrasonic spray coating showed homogeneous coatings after using UV-ozone and O_2 plasma treatment. The findings of this study provide valuable insights into the hydrocarbon airborne contamination on cleaned surfaces over time even in clean room environments and have a notable impact on the performance of liquid coatings and patterns. We highlight the importance of timing between the surface treatment and printing in achieving high-resolution or homogeneous.

1. Introduction

The treatment of substrate surfaces is extensively used in research spanning solar cells, biomedical sensors, production of micro- and nano-electronics [1-3]. To achieve homogeneous liquid thin films, the substrates must be clean and have a surface energy compatible with the ink. The evaporation rate of the solvent(s) should be in balance with the spreading of the liquid. A proper surface treatment can meet these requirements by removing organic and inorganic contaminants and modifying the surface [4]. However, over time the effect of the surface treatment

reduces due to interaction with the environment, resulting in a contaminated surface [5]. A poorly treated surface can cause de-wetting, resulting in inhomogeneous or incomplete covering liquid coatings. Droplet-based coating is a non-contact deposition technique that enables large area coating, with a low waste of material. However, it is limited by surface wetting and can produce capillary flows as well as so-called coffee rings of deposited particles [6]. Control of these effects would expand the usage of droplet based printing techniques.

Ultrasonic spray coating (USSC) is a technique that can be used to deposit functional thin coatings with a thickness of as low as 30 nm [7] on large and 3D substrates [8]. The small droplets generated by USSC have a narrow size range [9, 10], which allows homogenous coverage with minimal flow behavior of the deposited particles in the liquid thin film. However, the Marangoni flow inside a drying droplet will always be present, and fortunately, it can be minimized [11]. In order to minimize the Marangoni flow, the surface energy of the substrate should be high, which promotes the spreading of the deposited droplets.

Ink-jet printing, another droplet-based technique that can deposit thin functional films with sub-millimeter patterns [12] or cover full areas. The spreading and the resulting size of the deposited droplet are determined by the ink's surface tension, viscosity, and the surface energy of the substrate [13]. Therefore, using hydrophobic low surface energy surfaces, one can improve the printing resolution of ink-jet printing [14]. By modifying the substrate surface, making it more hydrophobic, one can therefore enhance the printing resolution.

Surface modification is crucial for achieving good results with droplet-based printing. Several dry cleaning techniques exist that can clean and modify the surface in different ways, such as UV-ozone, corona discharge, plasma (using gases such as O_2, CF_4, N_2, and Ar), and laser cleaning [5, 15-18]. The working principles of these methods are well understood. However, the

differences in surface modification result in different hydrocarbon contamination/degradation rates over time [5]. The effects of these surface modifications on glass are rather unclear. Knowing how the surface contamination evolves over time on glass after these modification techniques is crucial, especially for droplet-based printing such as ink-jet printing and ultrasonic spray coating. To study the contamination behavior and the differences between surface modification techniques, we investigated the treatment times for USSC and ink-jet printing. We use nanodiamond (ND) particles to study the importance of the surface modification [19-21]. Inadequate surface modification using various techniques can lead to issues such as surface roughness and the presence of surface residues as contamination or variations in surface energy. This leads to challenges such as uneven or poor layer deposition. As an example, Marangoni flows can occur in the case of particles like nanodiamond (ND) seeds, polystyrene nanoparticles [22] or even polymer films as PEIE or PEDOT:PSS for light emitting diodes[23, 24]. Importantly, there is a notable gap in the existing literature, particularly regarding the pretreatment for spray-coated/ink-jet printed layers on glass. The existing body of research lacks comprehensive studies addressing the specific requirements for effective nanodiamond seeding on glass substrates, encompassing both pretreatment methodologies and the characteristics of spray-coated/inkjet printed layers. Notably, there is a scarcity of published work investigating the impact of different pretreatment strategies on the homogeneity, adhesion, and optical properties of resulting nanodiamond layers. This gap highlights the need for a thorough exploration of these crucial aspects to establish a more robust foundation for applications on glass substrates. Addressing this gap not only contributes to the advancement of fundamental understanding but also holds significance for practical applications, such as improving the reliability and performance of nanodiamond coatings.

The deposited ND particles in the end are grown into coatings or patterns using chemical vapor deposition (CVD) [25]. The diamond coatings have a wide range of potential applications in fields such as biomedicine, optics, and electronics [26-28]. To investigate how the surface modification affects the ND seeding by USSC and ink-jet printing, we selected UV-ozone and O_2-plasma. UV-ozone does not require expensive vacuum pumps and is easily integrated into roll-to-roll production [29]. UV-Ozone and O_2 plasma are widely used in application-driven research but their exact influence on the deposition of nanoparticles on glass substrate is not described. If one would understand the influence of these pre-treatment techniques, the large-area deposition with ultrasonic spay coating, could be better optimized to reduce coffee rings and Marangoni flows[15, 22, 23]. On the other hand, inkjet printing of fine lines deserves a pre-treatment of the glass to enhance its hydrophobicity is beneficial; this can be achieved by CF_4 plasma cleaning. The same as for USSC, this treatment is known but the exact surface effects, taking into account the time of pre-treatment but also the time after pre-treatment (and before inkjet printing) is not described elsewhere.

2. Materials and Methods

2.1. Sample pre-treatment

Fused silica substrates (Neyco, France) with a size of 13 × 13 × 1 mm³ were wet-cleaned in an ultrasonic bath using Branson soap (for 5 min), deionized water (5 min), acetone and isopropanol for 10 min each and dried with nitrogen gas flow sequentially. In total 228 samples were divided into three sets, each set underwent a pre-treatment of UV-ozone, O_2-plasma, or CF_4-plasma. From each set one-half was used to measure the evolution of the contact angle (CA) over time for UV-ozone and O_2-plasma day after day for 21 days. The UV-ozone treatment was executed with a UV-ozone cleaner (Novascan PSD series). The CF_4-treated samples were measured the first single day at an interval of 1 hour 10 hours. The other samples were coated with ND seeds

using ultrasonic spray coating or patterned with NDs using ink-jet printing at the same time intervals. The samples treated using CF_4 plasma were ND seeded only with ink-jet printing in fine patterns, because due to hydrophobic surface they were not suitable for spray coating as it resulted in drastically not homogenous coatings.

The plasma treatments (O_2 and CF_4) were performed using a home-built system [5]. The vacuum chamber, configured horizontally, boasts a cylindrical geometry with a substantial diameter of 40 cm and an accommodating depth of 55 cm. Within this chamber, a 4-inch black carbon stage is positioned at a depth of 40 cm, for the placement of samples. This carbon stage, located at a height of 17 cm from the chamber base. To achieve the gas discharge plasma, the samples were biased negatively. The base pressure in the chamber was below 1.6×10^{-3} Pa. For O_2 plasma treatment the gas flow was 50 sccm and 200 W of power was applied for 2 min to generate the O_2 plasma, while for CF_4 plasma treatment the gas flow was 42 sccm and 300 W for 3 min was used. To achieve the gas discharge plasma the samples were biased negatively with 300 V and 340 V to generate O_2 and CF_4 plasma, respectively. The samples were placed on a carbon stage. One sample group was left untreated as a reference.

2.2. Diamond seeding

After the modification, samples were seeded with NDs using USSC and ink-jet printing. USSC (Exacta Coat, Sono-Tek cooperation) utilized the impact nozzle, the substrates temperature was kept at 90°C throughout the experiment and sprayed upon with an aqueous seeding suspension with 0.05 g/l (pH = 8.0) single-digit nanodiamonds (PlasmaChem GmbH). The suspension was atomized at 4 W power, and the flow rate was maintained at 0.25 mL/min. The nozzle to substrate distance was 5 cm and the shroud gas pressure of 9 kPa. The number of spray passes was 160 with a path speed of 50 mm/s.

The ND seeding in patterns with ink-jet printing was performed with a Fujifilm Dimatix DMP 2800 series drop-on-demand (DOD) ink-jet printer. Cartridges that eject 1 pL droplets were filled with a seeding solution of 55% ethylene glycol, 25% ethanol, and a 20% volume aqueous seeding suspension consisting of 3 g/l single-digit nano diamonds that were centrifuged at 5000 relative centrifugal force (RCF) for 30 min to remove the bigger ND clusters. Only one nozzle of the cartridge was used and droplets were ejected at 1 kHz frequency using pulses of 34 V (waveform as depicted as in figure S1(b)). On the hotplate the samples were heated to a temperature of 60°C. The samples were seeded by printing ND colloid droplets in two layers. In one layer a distance between the droplets of 30 µm was used. In total, two layers were shifted 5 µm to each other to print the pattern as shown in figure S1(a).

2.3 Diamond growth

After the seeding, nanocrystalline diamond (NCD) thin films of 200 nm were grown in the linear antenna microwave plasma-enhanced CVD system (LA MW PE CVD) [25]. In this system, the generated microwaves are delivered into the chamber by two four-paired coaxial antennas in quartz tubes, and powered with a continuous mode operation with a total microwave power of 5600 W. A base pressure of 0.01 Pa was used before filling the chamber with hydrogen, methane, and carbon dioxide gas with a gas flows of 133.5 sccm, 7.5 sccm and 9 sccm, respectively. During the CVD of 175 min, which resulted in a 200 nm thick NCD film, the substrate stage was heated to 400°C and kept at a 5 cm distance from the linear antennas.

2.4 Characterization

After the growth, optical microscopy images were made using a Zeiss Axiovert 40 MAT microscope combined with a Zeiss Axiocam 305 camera to inspect defects on a millimeter scale. A more detailed sub-micrometer inspection was done using the FEI Quanta 200 FEG scanning electron microscope (SEM).

Half of the samples were not seeded and were examined for contamination by measuring the contact angle (CA). The CA were evaluated by the sessile drop technique using an OCA 35, from DataPhysics Instruments, setting 0.5 μL droplets in four different location of each sample (Figure S7). The median value of these four different measurements was taken to reduce the effect of outliers The sample roughness was evaluated with an atomic force microscopy (AFM) Bruker Multimode 8 in tapping mode and a JPK-Bruker NanoWizard 3 AFM system. The X-ray Photoelectron Spectroscopy (XPS) analysis was conducted using a Physical Electronics PHI-5600LS electron spectrometer. Al-k alpha photons (1486.6 eV) from a monochromator system with a 1 mm spot size were utilized for the acquisition of survey and core-level spectra. The energy resolution of the spectrometer for core-level spectra was configured to 0.36 eV FWHM, encompassing both photon and electron contributions. Core-level spectral deconvolution was conducted using CasaXPS software, utilizing either Shirley or linear backgrounds. The analytical approach involved a numerical least-squares fitting process, aligning with Wertheim's method[30]. To address surface charging, charge compensation was facilitated using a Kimball Physics Inc. ELG-2 electron gun, setting the C 1s peak at 284.6 eV.

3. Results and discussions

3.1 Surface morphology

The surface root mean-square roughness (R_q) of the fused silica samples is shown in Figure 1(a) for the different treatments.

After the UV-ozone surface treatment, the surface roughness was reduced to (bare glass substrate with R_q of (1.3 ± 0.2) nm). By increasing the treatment time from 15 min to 60 min the surface was smoothed from (1.1 ± 0.1) nm to (0.7 ± 0.1) nm. A longer treatment time of 120 min etched deeper with increase of surface roughness to an average of (0.9 ± 0.1) nm. The UV-ozone

treatment roughens the surface linearly by (0.2±0.01 nm/h) after reaching the minimum roughness, indicating that at this point, all contaminations have been successfully etched away. Beyond this point, the etching process exclusively affects the glass(Figure S4). Etching occurs as a result of chemical reactions between oxygen radicals and the substrate [16]. The gas discharge plasma is more reactive. The samples were significant roughened to (3.3 ± 0.2) nm and (11.1 ± 0.3) nm R_q respectively for O_2 and CF_4 plasma.

3.2 Evolution of the contact angle and the surface wetting.

The surface contamination over time is investigated measuring the CA after the treatment after various time periods on UV-ozone, O_2, and CF_4 plasma treated samples.

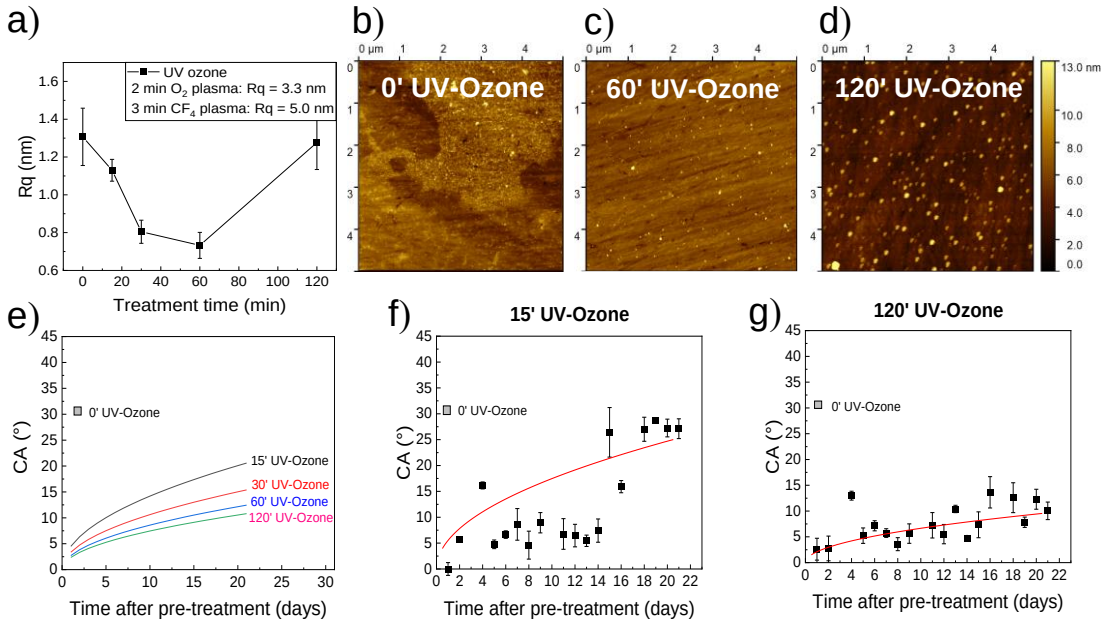

Fig. 1: (a) Surface roughness measured after different treatments with O_2, CF_4 plasma, 0, 15, 30, 60, and 120 min UV-ozone. (b) reference sample without treatment, (c) 60 min, and (d)120 min UV- ozone treatment. By having different etching rates or treatment times different roughness's can be achieved. (e) Evolution of CA after the UV-ozone pre-treatment for times of 0, 15,30, 60 and 120 min in fitted lines out of the data. The evolution of contact angles measured on (f) 15 min, and (g) 120 min treated samples.

The CA of an untreated sample is (30.6 ± 0.05) (Fig. 2). UV-ozone treatment makes the surface hydrophilic, but the duration of the treatment affects the amount of removed hydrocarbon contamination (Table S1). Clear differences between the treatment times can be seen in the fitted data (Fig. 1 (e)). The longer the treatment time, the lower the CA and also the higher the roughness (Fig. 1 (b-d)) (Figure S3). Observed results over 21 days shows that the CA increases over time due airborne hydrocarbon contamination (Fig. 2 (d), Table S1), and the spread in CA is smaller for the 120 min treated samples (Fig. 1 (g)). The saturation CA varies between the samples, with the longest treatment time (120 minutes) resulting in the lowest CA of (10.0 ± 1.7) and the least variation over the measured time of 21 days, Fig. 1 (f) and Fig. *1*1 (g). The saturation CA for 15, 30, and 60 minutes of treatment are (27 ± 1.9°), (11.1 ± 1.6), and (9.4 ±3.4°) degrees Fig. 1 (e) (Figure S1), respectively. Therefore, it is recommended to use treatment times of 60 or 120 minutes for most consistency.

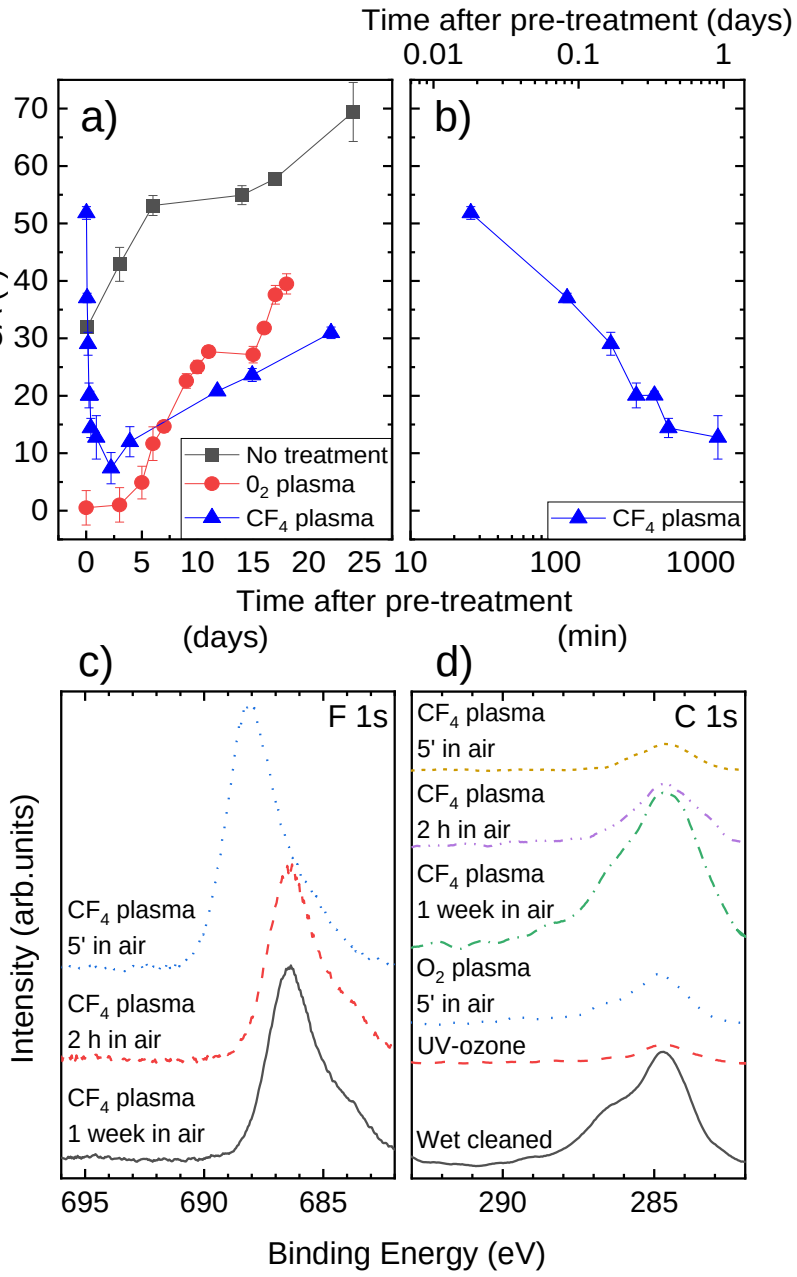

Fig. 2: *Evolution of CA (a) after no, O_2- , and CF_4- plasma treatment, (b) the evolution of the contact angle of CF_4-plasma treated samples in logarithmic scale in a timeframe zoomed in to 1* day and *(c) and (d) present the XPS C 1s and F 1s core-level spectra for samples subjected to wet cleaning, 60' UV-ozone, O_2-plasma, and CF_4-plasma treatments. Notably, the samples treated with CF_4 plasma were exposed to air for varying durations—1 week, 2 hours, and 5 minutes. These plots highlight the dynamic*

changes in fluorine and carbon content under different treatment conditions, revealing crucial details about their chemical evolution over time.

The Contact Angle (CA) measurements for O_2 plasma-treated samples display a smaller average standard deviation (1.6°) compared to those treated with UV-ozone (1.9°). Initially hydrophilic (CA < 4°), the O_2 plasma-treated samples undergo a marked transition to hydrophobicity within 3 to 4 days, as illustrated in Fig. 2 (a). This change, characterized by a sharp increase in CA, is attributed to airborne hydrocarbon contamination, detailed in Fig. 2 (d). After 19 days, the CA reaches (39.5 ± 1.8)°.

In contrast, CF_4 plasma-treated samples exhibit initial hydrophobicity with a CA of 51.8° ± 1.1° (*Fig. 2* (b)). However, within 10 hours, these surfaces become more hydrophilic (14.4° ± 1.7°), a change due to the oxidation-induced removal of most fluorine atoms, as evidenced by the rapid decline in CA within the first 24 hours (*Fig. 2* (c)). This trend confirms the fast or easy removal/oxidation [31] of the thin fluorine-terminated film formed during CF_4 plasma treatment, as shown in Figure S8. XPS analysis further reveals that the initial water contact angle on freshly CF_4-terminated substrates is about 51°, correlating with a limited fluorine coverage of 18.4% (Table S1). This effect is largely due to the high oxygen content in the fused silica glass (*Fig. 2* (b)). Notably, on fused silica glass substrates, a time-dependent reduction in fluorine content was observed. After 2 hours, the fluorine content decreased to 8.47%. Simultaneously, a notable presence of 4.60% carbon was detected after one week, indicating hydrocarbon contamination of the surface (Fig. 2 (d), Table S1). These findings underscore the dynamic evolution of surface properties over time, influenced by substrate composition and environmental factors. The observed changes in fluorine and carbon content contribute valuable insights into the temporal behavior of surface characteristics. Due to the increase of airborne hydrocarbon contamination

after 2 days, the CA starts to increase further, similar to the UV ozone and O_2 plasma treated samples. The hydrophobic behavior after the CF_4 termination is ideal for patterning with ink-jet printing where more hydrophobic surfaces are required. In contrast, it takes 20 days for O_2 plasma to achieve a higher CA. To avoid this long waiting times, no surface treatment is not an option, because it results in a surface with remained inhomogeneous contaminations. For this reason, CF_4 plasma surface termination is highly interesting for fine-line printing as it achieves higher CA immediately after the surface treatment.

3.3 ND seeding by ink-jet printing

At the time interval of one day after the UV-Ozone and the O_2 plasma treatment, the ND seeding on the samples was done using ink-jet printing.

To evaluate the resolution, edge conformity and the ND seeds flow behavior, the NCD thin films (200 nm) (*Fig. 3*) were grown over the comb pattern printed by ink-jet printer. The comb pattern consisted of lines with decreasing spacing from 140 µm to 20 µm in 20 µm steps, which allowed for an assessment of the precision in line spacing at different values.

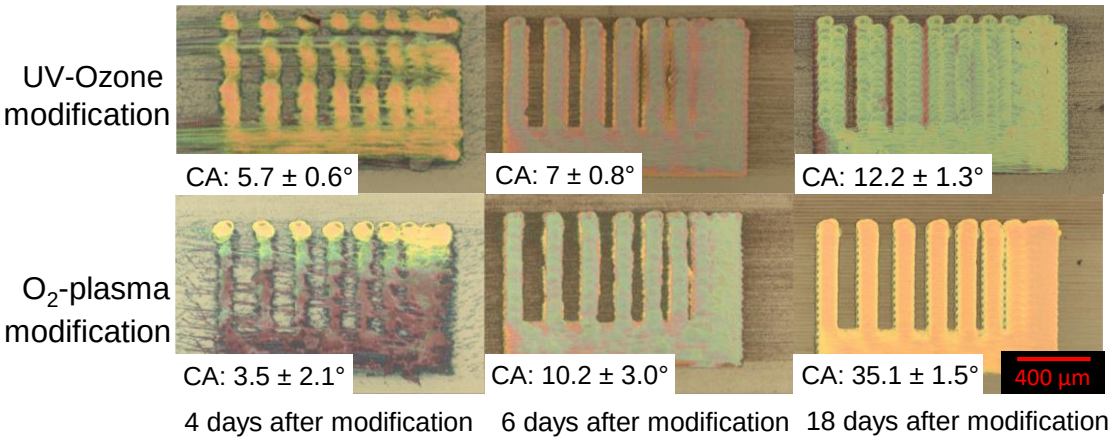

Fig. 3: Illustration of an ink-jet printed comb pattern, printed horizontally from right to left. The presented results correspond to samples subjected to 30' UV-Ozone and O_2 plasma treatments, with

observations taken at time intervals of 4, 6, and 18 days. These specific time points were selected to capture transitional moment.

Ink-jet printing on hydrophilic surfaces results in outflow of the ink and an undesirable pattern or surface (Figure S5) is achieved. This still happens with a contact angles of 5.7±0.6°° on samples that were kept in ambient conditions for 4 days. Samples kept in ambient for 6 days after 30' UV-ozone and O_2-plasma treatment the outflow is even reduced after 18 days due to the further increase in CA. Using O_2-plasma, sharper lines were achieved, e.g. The lines with an intermediate distance of 40 µm did not merge on the sample with CA of 35.1±1.5°, which is due to the higher roughness of the surface.

Using UV-ozone or O_2-plasma, CA of 9° are required (waiting times of at least 6 days) to avoid outflow of the ink. With CF_4-plasma, hydrophobic surfaces are achieved directly after the surface treatment (Fig. 2).

The maximum printing resolution achievable depends on the ability to control the droplet spreading and contact angle of the printed droplet after coalescence. [14, 32]. Therefore, single droplets were printed, and spreading and flow behavior inside the deposited droplet was evaluated (*Fig. 4*). With controlling the spreading and contact angle of the printed droplet, the final droplet size can be adjusted. The homogeneity of ND seed deposition can be adjusted by controlling the flow behavior inside the droplet, ranging from deposition of ND seeds in a ring to fully covered circles.

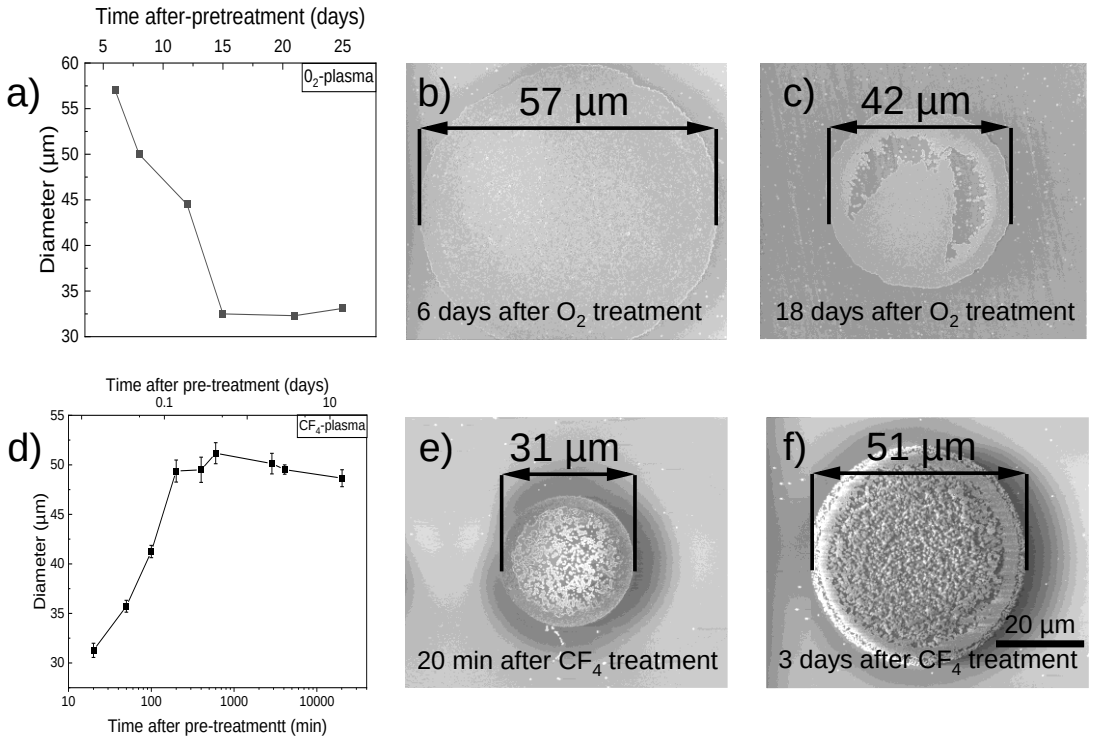

Fig. 4: The evolution of the diameter of multiple ink-jet-printed droplets as a function of the time after (a) O_2 plasma and (d) CF_4 plasma pre-treatment. The resulting droplet after 6 days (b), and 18 days (c) for O_2 plasma. 20 min (e) and 3 days (f) for CF_4 plasma.

Using CF_4, high resolution patterns can be achieved directly. This makes CF_4 plasma fast and interesting for in line productions in the industry. Moreover, samples should be printed within 2 h, to still profit from the hydrophobic like nature of the CF_4 plasma treatment with a CA higher than CA of the untreated glass. This all results in the fact that the single deposited droplet size can be regulated by varying the time between treatment and printing because of the change of CA. An increase of droplet diameter is observed starting with a diameter of 31 ± 1 µm after 20 min using the CF_4 plasma treatment. With more hydrophobic surfaces, even smaller deposited droplet sizes can be achieved. When higher printing CA are used, the nano diamond seeds can exhibit capillary-driven flow behavior during the printing process, resulting in the formation of a

coffee ring pattern[6]. This pattern causes the seeds to accumulate more densely at the edges of the ring, while the center of the ring has a sparser distribution of seeds (*Fig. 4*). Therefore, the CA plays a significant role in determining the quality and uniformity of the resulting diamond film. However, to achieve homogeneous surfaces the tendency of more hydrophilic surface are desired, which is the trade-off between homogeneous coverage and high resolution patterning.

3.4 ND seeding by ultrasonic spray coating

USSC seeded samples were evaluated after NCD growth. The homogeneity of the surfaces were evaluated using the micrographics obtained by SEM (Figure S6) and an optical microscope (*Fig. 5*). This evaluation was performed on samples seeded with different time intervals after the treatment using UV-ozone and O_2 plasma.

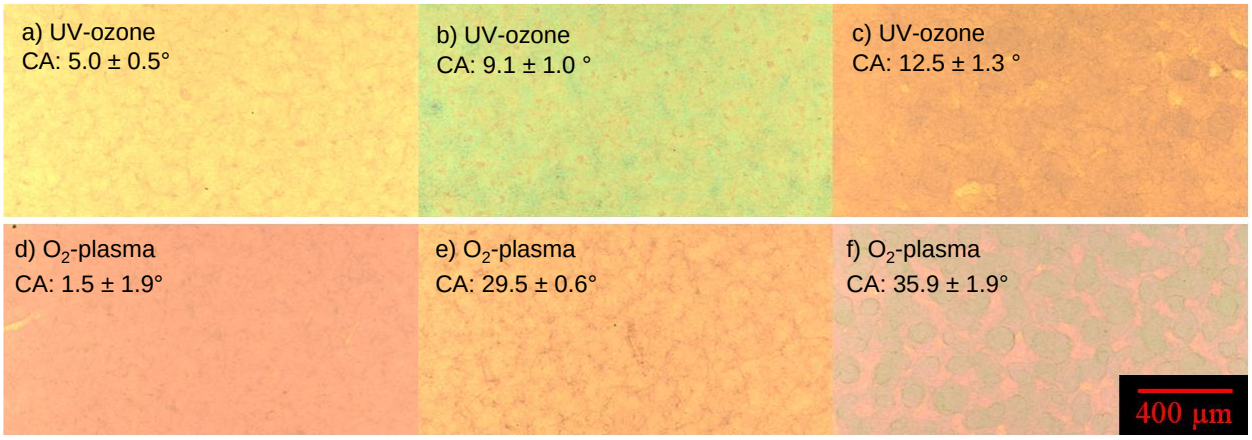

Fig. 5: Optical microscope images of samples with a grown NCD film. The samples were cleaned with 30' UV-ozone (a), (b), (c) and O_2-plamsa (d), (e), (f) and seeded afterwards using USSC with a time in between of 3,10, and 19 days respectively the cleaning and the seeding.

The difference between 30' UV-ozone and O_2-plasma was clearly visible in Fig. 5. Both gave good results when the USSC coating was performed between 0 and 6 days after the pre-treatment (*Fig. 5*(a) and 5(d)). However, seeding after 19 days on O_2 plasma treated samples resulted in a

pronounced inhomogeneous NCD film homogeneity (Fig. 5 (f)). Due to the lower CA, this effect is less pronounced for the UV-ozone treated samples (Fig. 5 (c)).

3.5 Printing operation space

The findings on contamination together with the experiments on printability of ND seeds are mapped in a designed printing operation space in *Fig. 6* using ink-jet printing and USSC in different time frames between the printing and surface modification.

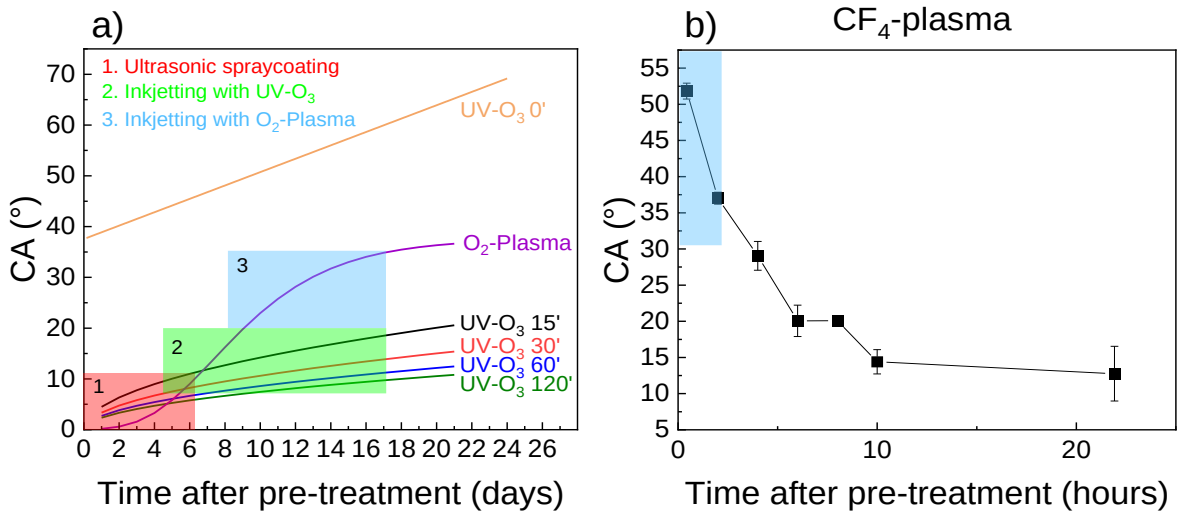

Fig. 6: Printing operation space for (a) UV-ozone and O_2-plasma and (b) for ink-jet printing on CF_4 plasma treated samples with their airborne contamination.

With USSC homogeneous surface coverage is desired. A substrate with as high as possible surface energy is advised. Therefore, it is optimal to print directly after the treatment of UV-ozone or O_2-plasma resulting in an operation space of 0 to 6 days (Fig. 6). Using ink-jet printing three different operation spaces where defined, one for each surface treatment technique. Using UV-ozone treatment, printing has to be executed in a timeframe of 4 to 16 days after the treatment. O_2-plasma cleaned samples need to be printed between 7 and 16 days after cleaning. For CF_4-plasma shorter waiting times are required, the samples have to be printed within 2 h. With reduced surface energy, high printing resolution can be achieved. When, with ink-jet

printing, homogeneous coverage of full surfaces is needed, one needs hydrophilic like surfaces in order to reduce the capillary driven flow behavior. For this, one can shift operation window to shorter times for UV-ozone and O_2-plasma modification. Resulting that, varying the times between surface modification and printing for UV-ozone, O_2 and CF_4 plasma terminated surfaces the resolution and the homogeneity of the print can be controlled with the mapped airborne contamination.

4 Conclusions

This study investigated how (i) different techniques for surface treatment affect the printability, (ii) airborne hydrocarbon contamination and other contaminants affect the surface over time. This directly influence the homogeneity of the print. Morphological differences were observed with UV-ozone, the treatment time has a significant influence on the final results. The UV-ozone gently etches the fused silica over time, resulting in higher roughness with over longer treatment times. The 15 min treatment time is too short, because the spread of contact angle values is significantly larger after 15 min treatment than after 60 min and 120 min treatment. Due the narrower spread of contact angle values already for a 60 min treatment, and the mild airborne hydrocarbon contamination rate, the 60 min UV-ozone treatment of fused silica is concluded to be optimal for nanodiamond seeding.

The reactive plasma O_2 and CF_4 plasma treatment, result in rougher surfaces with R_q of (3.3 ± 0.2) nm and (11.1 ± 0.3) nm respectively, due to the higher etching rate than in the case of UV-ozone treatment. Using O_2-plasma, because of the higher induced roughness, the final contact angle will be more hydrophobic-like with 35.9±1.9°° contact angle compared to the 30.6 ± 0.05 of the untreated surfaces. Due to the reactive treatment, the average spread of contact

angles is smaller (1.6°) than in the case of UV-ozone (1.9°) treated samples. Moreover, the surface stayed remained hydrophilic up to 3 days (CA < 4°).

CF_4-plasma treatment is concluded as a solution for ink-jet printing where hydrophobic surfaces are required for high-resolution printing. CA of 51.8±1.1° on fused silica was achieved due to the thin fluorocarbon film formation on the surface. High-resolution patterns with drop size diameters to 30 µm were demonstrated. On fused silica, only a thin film of fluorocarbon is created by CF_4 treatment, which quickly decays and thus hydrophobicity is lost within one day. In contrast after UV-ozone and O_2-plasma treatment one needs to wait several days before printing in order to achieve compatible results. However, this route is not reliable as it is difficult to control the rate of hydrocarbon contamination, which may depend on ambient conditions. Contrary if smooth homogeneous full layer coverages are desired with ND seed using USSC, UV-ozone and O_2-plasma are the best solutions.

One can conclude that UV-ozone and plasma modification are both methods to improve the wetting behavior of a liquid onto the surface of a substrate for printing.

The shown operation space in this work establishes the correlation between the different surface modification techniques in roughness and contact angles along with the printability and is therefore a powerful guideline and operation space for the right modification and optimized waiting times between modification and printing which can be used for full coatings or fine line patterning.

ASSOCIATED CONTENT

Supporting Information.

The Supporting Information is available at XXXXXXXXXXXX

AFM measured surface roughness images for different UV-ozone treatment times; Plot of UV-ozone etching rate; Optical microscope images of ink-jet printed samples; Scanning Electron Microscopy image; Contact angle measurement; X-ray Photoelectron Spectroscopy analysis

AUTHOR INFORMATION

Corresponding Author

Pieter Verding: Hasselt University, Institute for Materials Research (IMO-IMOMEC), Wetenschapspark 1, B-3590 Diepenbeek Belgium, E-mail: pieter.verding@uhasselt.be

Wim Deferme: Hasselt University, Institute for Materials Research (IMO-IMOMEC), Wetenschapspark 1, B-3590 Diepenbeek Belgium, Phone: +32-(0)11-268874,

E-mail: wim.deferme@uhasselt.be

Author Contributions

P.Verding, P. Podedinskas and W. Deferme designed and coordinated the research. W. Deferme, K. Haenen and P. Podedinskas supervised the work. D Reenaers, E Jeunen, and S Thomas seeded the samples with ink-jet printing and ultrasonic spray coating. R. M. Joy has grown the diamond thin film. P. Verding, processed, cleaned and characterized the samples and conducted SEM, cleaning, optical microscopy and contact angle analysis. Rachith S. N. and R

Rouzbahani conducted AFM measurements. P. Verding analyzed, interpreted all data and drafted the manuscript with aid from W. Deferme, P. Podedinskas. Hans-Gerd Boyen and Derese Desta contributed through the measurement and analysis of the XPS data. The manuscript was written through contributions and discussions with of all authors. All authors have given approval to the final version of the manuscript. The authors declare no competing financial interest.

Funding Sources

This work was partly funded by the Research Foundation-Flanders (FWO) via projects 1S99121N and G0D4920N, and the Methusalem NANO network.

ABBREVIATIONS

AFM: Atomic Force Microscopy, Ar: Argon, CA: Contact Angle, CO: Carbon Monoxide, CO_2:Carbon Dioxide, COF_2: Carbonyl fluoride, CF: Fluorocarbon, CF_2: Difluoro methylene, CF_3: Trifluoromethyl, CVD: Chemical Vapor Deposition, DOD: Drop on-demand ,H_2O: Water, N_2: Dinitrogen, ND: Nano diamond, O*: Oxygen radical, O_2: Oxygen

O_2^{2-}: Oxygen peroxide ion, O_3: Ozone, pH: Potential of hydrogen, RCF: Relative centrifugal force, RMS: Root Mean Square, SEM: Scanning Electron Microscopy, SiO_2: Silicon Dioxide, Sccm: Standard cubic centimeter per minute, UV: Ultraviolet, USSC: Ultrasonic spray coating, µl: Microliter, *hv*: *h* = Planck's constant, ν = frequency; XPS: X-ray photoelectron spectroscopy

REFERENCES

(1) Gupta, S. K.; Jindal, R.; Garg, A. Microscopic Investigations into the Effect of Surface Treatment of Cathode and Electron Transport Layer on the Performance of Inverted Organic Solar Cells. *Acs Applied Materials & Interfaces* **2015**, *7* (30), 16418-16427. DOI: 10.1021/acsami.5b03583.
(2) Saha, S.; Chan, Y. T.; Soleymani, L. Enhancing the Photoelectrochemical Response of DNA Biosensors Using Wrinkled Interfaces. *Acs Applied Materials & Interfaces* **2018**, *10* (37), 31178-31185. DOI: 10.1021/acsami.8b12286.

(3) Liu, J. S.; He, L. C.; Wang, L.; Man, Y. C.; Huang, L. Y.; Xu, Z.; Ge, D.; Li, J. M.; Liu, C.; Wang, L. D. Significant Enhancement of the Adhesion between Metal Films and Polymer Substrates by UV-Ozone Surface Modification in Nanoscale. *Acs Applied Materials & Interfaces* **2016**, *8* (44), 30576-30582. DOI: 10.1021/acsami.6b09930.
(4) Navas, J.; Araujo, D.; Piner, J. C.; Sanchez-Coronilla, A.; Blanco, E.; Villar, P.; Alcantara, R.; Montserrat, J.; Florentin, M.; Eon, D.; et al. Oxygen termination of homoepitaxial diamond surface by ozone and chemical methods: An experimental and theoretical perspective. *Applied Surface Science* **2018**, *433*, 408-418. DOI: 10.1016/j.apsusc.2017.10.065.
(5) Pobedinskas, P.; Degutis, G.; Dexters, W.; D'Haen, J.; Van Bael, M. K.; Haenen, K. Nanodiamond seeding on plasma-treated tantalum thin films and the role of surface contamination. *Applied Surface Science* **2021**, *538*. DOI: 10.1016/j.apsusc.2020.148016.
(6) Deegan, R. D.; Bakajin, O.; Dupont, T. F.; Huber, G.; Nagel, S. R.; Witten, T. A. Capillary flow as the cause of ring stains from dried liquid drops. *Nature* **1997**, *389* (6653), 827-829. DOI: 10.1038/39827.
(7) Kwon, S. I.; Kyung, K. H.; Park, J. Y.; Lee, I. S.; Kim, J. H.; Kim, S. H.; Shiratori, S. Uniform anti-reflective films fabricated by layer-by-layer ultrasonic spray method. *Colloids and Surfaces a-Physicochemical and Engineering Aspects* **2019**, *580*. DOI: 10.1016/j.colsurfa.2019.123785.
(8) van den Ham, E. J.; Elen, K.; Bonneux, G.; Maino, G.; Notten, P. H. L.; Van Bael, M. K.; Hardy, A. 3D indium tin oxide electrodes by ultrasonic spray deposition for current collection applications. *Journal of power sources* **2017**, *348*, 130-137. DOI: 10.1016/j.jpowsour.2017.03.006.
(9) Avvaru, B.; Patil, M. N.; Gogate, P. R.; Pandit, A. B. Ultrasonic atomization: Effect of liquid phase properties. *Ultrasonics* **2006**, *44* (2), 146-158. DOI: 10.1016/j.ultras.2005.09.003.
(10) Verding, P.; Deferme, W.; Steffen, W. Velocity and size measurement of droplets from an ultrasonic spray coater using photon correlation spectroscopy and turbidimetry. *Applied Optics* **2020**, *59* (25), 7496-7503. DOI: 10.1364/ao.402579.
(11) Raju, L. T.; Diddens, C.; Li, Y. X.; Marin, A.; van der Linden, M. N.; Zhang, X. H.; Lohse, D. Evaporation of a Sessile Colloidal Water-Glycerol Droplet: Marangoni Ring Formation. *Langmuir* **2022**, *38* (39), 12082-12094. DOI: 10.1021/acs.langmuir.2c01949.
(12) Nguyen, P. Q. M.; Yeo, L. P.; Lok, B. K.; Lam, Y. C. Patterned Surface with Controllable Wettability for Inkjet Printing of Flexible Printed Electronics. *Acs Applied Materials & Interfaces* **2014**, *6* (6), 4011-4016. DOI: 10.1021/am4054546.
(13) Park, J.; Han, H. S.; Kim, Y. C.; Ahn, J. P.; Ok, M. R.; Lee, K. E.; Lee, J. W.; Cha, P. R.; Seok, H. K.; Jeon, H. Direct and accurate measurement of size dependent wetting behaviors for sessile water droplets. *Scientific Reports* **2015**, *5*. DOI: 10.1038/srep18150.
(14) Kwon, J. S.; Lee, D. J.; Oh, J. H. Formation and Characterization of Inkjet-Printed Nanosilver Lines on Plasma-Treated Glass Substrates. *Applied Sciences-Basel* **2018**, *8* (2). DOI: 10.3390/app8020280.
(15) Aronsson, B. O.; Lausmaa, J.; Kasemo, B. Glow discharge plasma treatment for surface cleaning and modification of metallic biomaterials. *Journal of Biomedical Materials Research* **1997**, *35* (1), 49-73.
(16) Vig, J. R. UV OZONE CLEANING OF SURFACES. *Journal of Vacuum Science & Technology a-Vacuum Surfaces and Films* **1985**, *3* (3), 1027-1034. DOI: 10.1116/1.573115.

(17) Zehner, D. M.; White, C. W.; Ownby, G. W. PREPARATION OF ATOMICALLY CLEAN SILICON SURFACES BY PULSED LASER IRRADIATION. *Applied Physics Letters* **1980**, *36* (1), 56-59. DOI: 10.1063/1.91315.
(18) Ryu, J.; Wakida, T.; Takagishi, T. EFFECT OF CORONA DISCHARGE ON THE SURFACE OF WOOL AND ITS APPLICATION TO PRINTING. *Textile Research Journal* **1991**, *61* (10), 595-601. DOI: 10.1177/004051759106101006.
(19) Chen, Y. C.; Tzeng, Y.; Cheng, A. J.; Dean, R.; Park, M.; Wilamowski, B. M. Inkjet printing of nanodiamond suspensions in ethylene glycol for CVD growth of patterned diamond structures and practical applications. *Diamond and Related Materials* **2009**, *18* (2-3), 146-150. DOI: 10.1016/j.diamond.2008.10.004.
(20) Sartori, A. F.; Belardinelli, P.; Dolleman, R. J.; Steeneken, P. G.; Ghatkesar, M. K.; Buijnsters, J. G. Inkjet-Printed High-Q Nanocrystalline Diamond Resonators. *Small* **2019**, *15* (4). DOI: 10.1002/smll.201803774.
(21) Verding, P.; Pobedinskas, P.; Joy, R. M.; Ahmed, E.; Remes, Z.; Kumar, R. S. N.; Baron, S.; Hofer, M.; Sittinger, V.; Nesladek, M.; et al. The influence of droplet-based seeding of nanodiamond particles on the morphological, optical, and mechanical properties of diamond coatings on glass. *Surface & Coatings Technology* **2023**, *459*. DOI: 10.1016/j.surfcoat.2023.129391.
(22) Stryckers, J.; D'Olieslaeger, L.; Silvano, J. V. M.; Apolinario, C. K.; Laranjeiro, A. C. G.; Gruber, J.; D'Haen, J.; Manca, J.; Ethirajan, A.; Deferme, W. Layer formation and morphology of ultrasonic spray coated polystyrene nanoparticle layers. *physica status solidi (a)* **2016**, *213* (6), 1441-1446. DOI: https://doi.org/10.1002/pssa.201533026.
(23) Verboven, I.; Nithyanandakumar, R. S.; Van Landeghem, M.; Pellaers, H.; Ruttens, B.; D'Haen, J.; Vandewal, K.; Deferme, W. Ultrasonic spray coating of polyethylenimine (ethoxylated) as electron injection and transport layer for organic light emitting diodes: The influence of layer morphology and thickness on the interface physics between polyethylenimine (ethoxylated) and the Al cathode. *Nano Select* **2022**, *3* (4), 851-863. DOI: https://doi.org/10.1002/nano.202100235.
(24) Kumar, R. S. N.; Ramirez, A. V.; Verding, P.; Nivelle, P.; Renner, F.; D'Haen, J.; Deferme, W. Deposition of ultra-thin coatings by a nature-inspired Spray-on-Screen technology. *Communications Engineering* **2023**, *2* (1), 42. DOI: 10.1038/s44172-023-00093-0.
(25) Drijkoningen, S.; Pobedinskas, P.; Korneychuk, S.; Momot, A.; Balasubramaniam, Y.; Van Bael, M. K.; Turner, S.; Verbeeck, J.; Nesladekt, M.; Haenen, K. On the Origin of Diamond Plates Deposited at Low Temperature. *Crystal Growth & Design* **2017**, *17* (8), 4306-4314. DOI: 10.1021/acs.cgd.7b00623.
(26) Wang, X. C.; Wang, C. C.; Shen, X. T.; Sun, F. H. Potential material for fabricating optical mirrors: polished diamond coated silicon carbide. *Applied Optics* **2017**, *56* (14), 4113-4122. DOI: 10.1364/ao.56.004113.
(27) Pandey, P. C.; Shukla, S.; Pandey, G.; Narayan, R. J. Nanostructured diamond for biomedical applications. *Nanotechnology* **2021**, *32* (13). DOI: 10.1088/1361-6528/abd2e7.
(28) Latawiec, P.; Venkataraman, V.; Burek, M. J.; Hausmann, B. J. M.; Bulu, I.; Loncar, M. On-chip diamond Raman laser. *Optica* **2015**, *2* (11), 924-928. DOI: 10.1364/optica.2.000924.
(29) Hah, J.; Song, B.; Moon, K. S.; Graham, S.; Wong, C. P.; Ieee. Design and Surface Modification of PET Substrates using UV/Ozone Treatment for Roll-to-Roll Processed Solar Photovoltaic (PV) Module Packaging. In *68th IEEE Electronic Components and Technology*

Conference (ECTC), San Diego, CA, May 29-Jun 01, 2018; 2018; pp 2397-2403. DOI: 10.1109/ectc.2018.00361.
(30) Wertheim, G. K.; Dicenzo, S. B. LEAST-SQUARES ANALYSIS OF PHOTOEMISSION DATA. *Journal of Electron Spectroscopy and Related Phenomena* **1985**, *37* (1), 57-67. DOI: 10.1016/0368-2048(85)80082-7.
(31) Oehrlein, G. S.; Zhang, Y.; Vender, D.; Joubert, O. FLUOROCARBON HIGH-DENSITY PLASMAS .2. SILICON DIOXIDE AND SILICON ETCHING USING CF4 AND CHF3. *J. Vac. Sci. Technol. A-Vac. Surf. Films* **1994**, *12* (2), 333-344, Article. DOI: 10.1116/1.578877.
(32) Lemarchand, J.; Bridonneau, N.; Battaglini, N.; Carn, F.; Mattana, G.; Piro, B.; Zrig, S.; Noel, V. Challenges, Prospects, and Emerging Applications of Inkjet-Printed Electronics: A Chemist's Point of View. *Angewandte Chemie-International Edition* **2022**, *61* (20). DOI: 10.1002/anie.202200166.